Biophysical Journal Volume 83 November 2002 2767–2780

Calcium Binding to Calmodulin Mutants Monitored by Domain-Specific Intrinsic Phenylalanine and Tyrosine Fluorescence

Wendy S. VanScyoc,* Brenda R. Sorensen,* Elena Rusinova,† William R. Laws,‡ J. B. Alexander Ross,‡ and Madeline A. Shea*

*Department of Biochemistry, University of Iowa College of Medicine, Iowa City, Iowa 52242; †Department of Medicine, Mount Sinai School of Medicine, New York, New York 10029; and ‡Department of Chemistry, University of Montana, Missoula, Montana 59812 USA

ABSTRACT Cooperative calcium binding to the two homologous domains of calmodulin (CaM) induces conformational changes that regulate its association with and activation of numerous cellular target proteins. Calcium binding to the pair of high-affinity sites (III and IV in the C-domain) can be monitored by observing calcium-dependent changes in intrinsic tyrosine fluorescence intensity ($\lambda_{ex}/\lambda_{em}$ of 277/320 nm). However, calcium binding to the low-affinity sites (I and II in the N-domain) is more difficult to measure with optical spectroscopy because that domain of CaM does not contain tryptophan or tyrosine. We recently demonstrated that calcium-dependent changes in intrinsic phenylalanine fluorescence ($\lambda_{ex}/\lambda_{em}$ of 250/280 nm) of an N-domain fragment of CaM reflect occupancy of sites I and II (VanScyoc, W. S., and M. A. Shea, 2001, *Protein Sci.* 10:1758–1768). Using steady-state and time-resolved fluorescence methods, we now show that these excitation and emission wavelength pairs for phenylalanine and tyrosine fluorescence can be used to monitor equilibrium calcium titrations of the individual domains in full-length CaM. Calcium-dependent changes in phenylalanine fluorescence specifically indicate ion occupancy of sites I and II in the N-domain because phenylalanine residues in the C-domain are nonemissive. Tyrosine emission from the C-domain does not interfere with phenylalanine fluorescence signals from the N-domain. This is the first demonstration that intrinsic fluorescence may be used to monitor calcium binding to each domain of CaM. In this way, we also evaluated how mutations of two residues (Arg74 and Arg90) located between sites II and III can alter the calcium-binding properties of each of the domains. The mutation R74A caused an increase in the calcium affinity of sites I and II in the N-domain. The mutation R90A caused an increase in calcium affinity of sites III and IV in the C-domain whereas R90G caused an increase in calcium affinity of sites in both domains. This approach holds promise for exploring the linked energetics of calcium binding and target recognition.

INTRODUCTION

Calmodulin (CaM) is a ubiquitous calcium sensor in all vertebrate cells. It regulates a large number of target proteins including kinases, phosphatases, metabolic enzymes, ion channels, and transcription factors (Carafoli and Klee, 1999). Changes in cellular calcium concentration during signal transduction cause CaM to modulate the activity of these targets differentially. The mechanism of target activation by CaM is dependent on the ion-binding properties of its four EF-hand calcium-binding sites, two in each domain (Fig. 1 *A*) (Babu et al., 1988; Chattopadhyaya et al., 1992) and the structural rearrangements that are induced by binding (Crivici and Ikura, 1995). Calcium binding results in exposure of hydrophobic clefts (LaPorte et al., 1980) and reorientation of the four helices in each domain (Strynadka and James, 1989; Nelson and Chazin, 1998; Yap et al., 1999). By inspection of the internal sequence homology within CaM, the N-domain is composed of residues 1–75, and the C-domain is composed of residues 76–148 (Fig. 1 *B*). However, despite their structural similarity, the highly homologous domains are not equivalent in calcium-binding energetics. The C-domain sites (III and IV) have a 10-fold higher affinity for calcium than the N-domain sites (I and II). Therefore, sites in the C-domain are filled almost completely before sites in the N-domain begin to be occupied (Seamon, 1980; Ikura et al., 1983; Klevit et al., 1984; Wang, 1985).

We are interested in understanding the determinants of differences between the calcium-binding properties of each of the four sites in CaM. It has been recognized for many years that increases in fluorescence intensity of Y138, one of the two tyrosine residues in the C-domain, can be used to resolve the free energies of calcium binding to sites III and IV (Richman and Klee, 1979; Klevit, 1983; Larson et al., 1990; Ross et al., 1992). Monitoring free energies of calcium binding to sites I and II in CaM has been more difficult because there are no tryptophan or tyrosine residues in the N-domain. Some methods for measuring equilibrium calcium-binding properties of the N-domain, including flow dialysis (Haiech et al., 1980, 1981; Buccigross et al., 1986; Gilli et al., 1998), discontinuous equilibrium titrations monitored by NMR (Pedigo and Shea, 1995a), or proteolytic footprinting (Sorensen and Shea, 1998; Shea et al., 2000) require extensive dialysis and large quantities of protein. Other methods require modifications to CaM, including engineered tryptophan residues (Kilhoffer et al., 1992; Martin et al., 2000; Ababou and Desjarlais, 2001; Tikunova et al., 2001) and side-chain modification (Nomura et al., 1992; Yao et al., 1994), which may perturb calcium-binding prop-

Submitted November 29, 2001, and accepted for publication June 26, 2002.

Address reprint requests to Dr. Madeline A. Shea, 51 Newton Road, Rm. 4-403 BS, Iowa City, IA 52242-1109. Tel.: 319-335-7885; Fax: 319-335-9570; E-mail: madeline-shea@uiowa.edu.

0006-3495/02/11/2767/14 $2.00

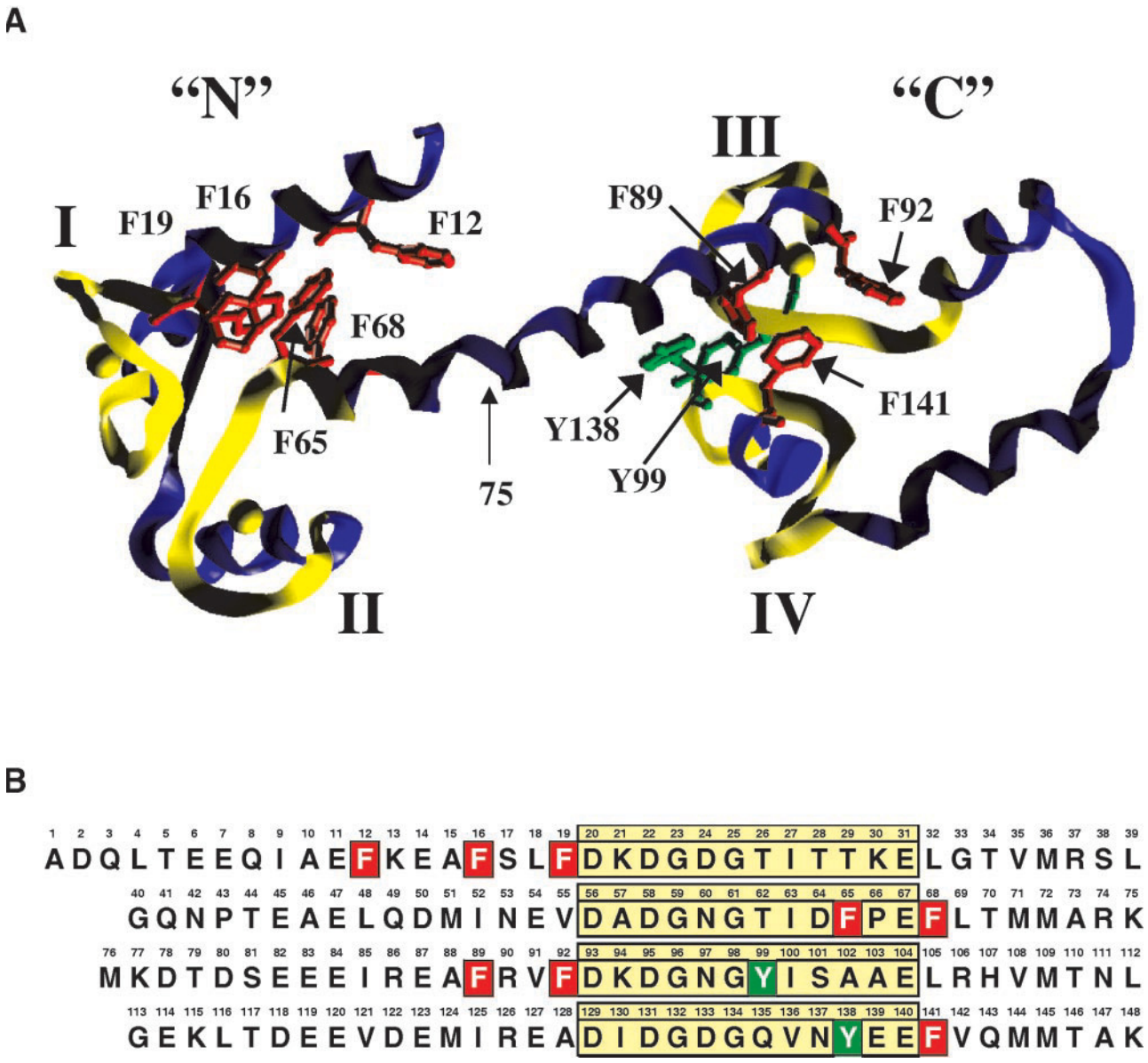

FIGURE 1 Rat calmodulin. (*A*) Ribbon diagram (SYBYL, Tripos Associates, St. Louis, MO) of calcium-saturated CaM (3CLN.pdb) (Babu et al., 1988); (*B*) Amino acid sequence showing calcium-binding sites I–IV in yellow and positions of tyrosine in green and phenylalanine in red.

erties. Stoichiometric titrations of calcium binding to CaM in competition with independently characterized chromophoric calcium indicators (Martin et al., 1985, 1996; Linse et al., 1991; Waltersson et al., 1993; Malmendal et al., 1999) may be used to estimate macroscopic (i.e., Adair) equilibrium constants. However, this approach directly monitors the fractional saturation of the indicator dye rather than CaM and requires coordinated analysis of CaM fragments to assign the macroscopic constants to individual domains. It also is very sensitive to precise determinations of the protein concentration and levels of contaminating calcium.

The N-domain of CaM contains five phenylalanine residues, and a calcium-dependent change in phenylalanine fluorescence intensity has provided a way to determine free energies of calcium binding to sites I and II of a half-molecule N-domain fragment, $CaM_{(1–75)}$ (VanScyoc and Shea, 2001). In this study, we asked whether binding to sites I and II could still be observed and resolved within full-length CaM, $CaM_{(1–148)}$, by monitoring the calcium-dependent change in phenylalanine fluorescence. Potential interference could be due to fluorescence from the three phenylalanine residues in the C-domain (positions 89, 92, and 141) as well as from the two tyrosine residues (positions 99 and 138) in the C-domain. In addition, fluorescence of N-domain phenylalanine residues might be quenched through perturbation of their local environments induced by domain-domain interactions or through energy transfer to C-domain tyrosine residues.

Here, using steady-state and time-resolved fluorescence studies, we show that phenylalanine fluorescence can be used selectively to monitor calcium binding to sites I and II of $CaM_{(1–148)}$. Therefore, calcium binding to both domains can be monitored easily in a single continuous titration by using tyrosine fluorescence (λ_{ex} = 277 nm; λ_{em} = 320 nm) as the reporter for sites III and IV (Richman and Klee, 1979; Klevit, 1983; Larson et al., 1990; Ross et al., 1992) and phenylalanine fluorescence (λ_{ex} = 250 nm; λ_{em} = 280 nm) as the reporter for sites I and II. Using these wavelength pairs and the optical conditions described here, there was no signal overlap between the two reporters. In addition, the phenylalanine residues in the C-domain were not emissive. Their quenching, at least in part, could be due to energy transfer to the nearby tyrosine residues.

We apply this approach to study how mutation of two residues between calcium-binding site II of the N-domain and site III of the C-domain affect the calcium affinities of one or both domains. The use of intrinsic, domain-specific probes opens the way for exploring effects of additional mutations on CaM and the physiological function of CaM as a regulator of a diverse array of cellular target proteins.

MATERIALS AND METHODS

Chemicals

All chemicals were reagent grade.

Overexpression and purification of calmodulin

Rat calmodulin ($CaM_{(1–148)}$), complementary domain fragments $CaM_{(1–75)}$ (N-domain) and $CaM_{(76–148)}$ (C-domain), and full-length mutants, $R74A_{(1–148)}$, $R90G_{(1–148)}$, and $R90A_{(1–148)}$ were cloned and overexpressed by standard methods (Sorensen and Shea, 1998). The proteins were purified as described by Putkey et al. (1985). The recombinant proteins were 97–99% pure as judged by silver-stained SDS-polyacrylamide gel electrophoresis or reversed-phase high-performance liquid chromatography. Amino acid analyses were conducted by the Molecular Analysis Facility at the University of Iowa College of Medicine.

Steady-state fluorescence excitation and emission spectra

Spectra were collected at 22°C using an SLM 4800C fluorometer (SLM Instruments) with a xenon short arc lamp (Ushio). Emission and excitation spectra of all samples (6 μM) in apo buffer (50 mM HEPES, 100 mM KCl, 0.05 mM EGTA, and 5 mM nitrilotriacetic acid (NTA), pH 7.40) and calcium-saturated buffer (apo buffer with 10 mM $CaCl_2$) were collected in 1-nm increments using 8-nm bandpasses. A matching buffer scan (blank) was subtracted from each spectrum. Spectra were not corrected for the response of the instrument.

Time-resolved fluorescence

Fluorescence intensity decay curves were collected void of depolarizing effects by exciting samples with vertically polarized light and observing the fluorescence through a polarizer oriented at the magic angle (Lakowicz, 1999). These experiments were performed by time-correlated, single-photon counting. Pulses, ~2 ps wide (full width at half-maximum), occurring at 4.8 MHz, were generated by a laser system (Verdi V10, Mira 900, and pulse picker 9200 from Coherent, Santa Clara, CA; harmonic generator 5-050 from Inrad, Northvale, NJ) tuned to the desired excitation wavelength. The sample was maintained at 20°C in an automated sample chamber (FLASC1000 from Quantum Northwest, Spokane, WA). Emitted photons were first selected for their polarization by an emission polarizer oriented at the magic angle (54.7°) and then for their energy by a monochromator (SpectraPro-150 from Acton, Acton, MA) with a bandpass of 10 nm and were detected by a module containing a photomultiplier tube, preamplifier, and constant fraction discriminator (TBX-04 from IBX, Glasgow, UK). The time between each excitation and emission event was processed by electronics (EG&G Ortec, Oak Ridge, TN) to collect a histogram of the probability of decay into 2048 channels (24 ps/channel). Instrument response functions (light scatter) and decay curves typically were collected to 100,000 and 40,000 counts in the peak, respectively.

Intensity decays, $I_M(t)$, were fit to a sum of exponentials.

$$I_M(t) = \frac{1}{3}\sum_{i=1}^{n} \alpha_i e^{-t/\tau_i}, \quad (1)$$

where the τ_i represent fluorescence lifetimes and the α_i are preexponential weighting factors, by a standard reconvolution procedure (Grinvald and Steinberg, 1974) using nonlinear least-squares regression (Bevington, 1969). All fits were judged by the reduced χ^2, the weighted residuals, and the autocorrelation of the residuals. Joint support plane confidence intervals were calculated for all iterated parameters by the approximation method described by Johnson and coworkers (Straume et al., 1991). To help assess whether different proteins had related intensity decay behavior, global analyses (Beechem et al., 1983; Knutson et al., 1983) were performed where it was assumed that the fluorescence lifetimes were excitation and emission wavelength independent and common to all datasets.

Equilibrium calcium titrations

Macroscopic binding constants for calcium binding to sites I and II and/or sites III and IV were determined by titrating the CaM proteins (6 μM in 50 mM HEPES, 100 mM KCl, 0.05 mM EGTA, and 5 mM NTA buffer, pH 7.4, at 22°C) as described previously (Sorensen and Shea, 1998). Binding to sites I and II was monitored by phenylalanine fluorescence using excitation at 250 nm and emission at 280 nm with 8-nm bandpasses. Binding to sites III and IV was monitored by tyrosine fluorescence using excitation at 277 nm and emission at 320 nm with 8-nm bandpasses. Free calcium concentration at each point in the titration was determined by the extent of saturation of the calcium indicator dye Oregon Green 488 BAPTA-5N (0.1 μM; Molecular Probes, Eugene, OR; see Eq. 2).

$$[\text{Calcium}]_{\text{free}} = K_d \frac{f_{[\text{high}]} - f_{[X]}}{f_{[X]} - f_{[\text{low}]}} \quad (2)$$

The K_d for Oregon Green was determined to be 29.6 μM in 50 mM HEPES, pH 7.4, with 100 mM KCl at 22°C. Using an indicator dye to determine free calcium concentration and a calcium buffering system (EGTA and NTA) minimizes the effect of small uncertainties in the concentration of protein and calcium titrant solution. Analysis of free energies of calcium binding to sites I and II (phenylalanine fluorescence) or to sites III and IV (tyrosine fluorescence) was performed by fitting the titration data to a model-independent two-site (Adair) function (Eq. 3) as described previously (Sorensen and Shea, 1998; Shea et al., 2000; VanScyoc and Shea, 2001):

$$\bar{Y} = \frac{K_1[X]^1 + 2K_2[X]^2}{2(1 + K_1[X]^1 + K_2[X]^2)} \quad (3)$$

The free energy of calcium binding to both sites in a domain is given by ΔG_2 ($-RT \ln(K_2)$. All titrations were repeated at least three times; representative data and fitted curves are shown in Figs. 3 and 4. The robustness of this approach was demonstrated by conducting titrations of sites III and IV in $CaM_{(76-148)}$ at two protein concentrations (1 μM and 6 μM), and nonlinear least-squares analysis gave free energies of calcium-binding identical to within the noise of an individual titration (data not shown).

An estimate of the lower limit of the free energy of cooperativity (ΔG_c) between paired calcium-binding sites within each domain was determined by Eq. 4 (see Pedigo and Shea, 1995b, for discussion).

$$\Delta G_c = \Delta G_2 - 2\Delta G_1 - RT \ln(4) \quad (4)$$

RESULTS

Steady-state fluorescence

A series of excitation and emission spectra were obtained for $CaM_{(1-148)}$ and its domain fragments $CaM_{(1-75)}$ and $CaM_{(76-148)}$. To evaluate contributions from the aromatic residues, different fixed wavelengths were used. To measure excitation spectra, an emission wavelength of 280 nm (Fig. 2, *A–C*) was used for phenylalanine, and 320 nm (Fig. 2, *D–F*) was used for tyrosine. Likewise, emission spectra were collected with excitation at 250 nm (Fig. 2, *G–I*) for phenylalanine or 277 nm (Fig. 2, *J–L*) for tyrosine.

The spectra for amino acids phenylalanine and tyrosine (Fig. 2, *A*, *D*, *G*, and *J*) did not change by addition of calcium (not shown). As shown in Fig. 2, *B* and *H*, the maximum fluorescence intensity from the phenylalanine residues in $CaM_{(1-75)}$ was quenched ~70% by the addition of calcium. Excitation spectra for the apo and calcium-bound forms of $CaM_{(76-148)}$ did not vary significantly (Fig. 2 *B*). Fig. 2 *H* demonstrates that the tyrosine residues in $CaM_{(76-148)}$ were excited at 250 nm. The addition of saturating calcium increased emission approximately threefold. However, there was little or no fluorescence detected at 280 nm (see bar in Fig. 2 *H*) for either apo or calcium-saturated $CaM_{(76-148)}$. The shapes and energies of these spectra were essentially the same as those of the reference amino acids.

Spectra for full-length CaM are shown in Fig. 2, *C* and *I*. Upon saturation by calcium, a decrease in phenylalanine emission (~70%) and an approximately threefold increase in tyrosine emission was observed. The spectra for both the apo and calcium-bound forms of the full-length CaM showed contributions from the corresponding spectra of the individual domains (Fig. 2, *B* and *H*).

Fig. 2, *E* and *K*, demonstrate that, with excitation at 277 nm, tyrosine fluorescence increased approximately threefold upon calcium binding to $CaM_{(76-148)}$. There was no fluorescence detected from $CaM_{(1-75)}$. Consequently, the spectra for the apo and calcium-bound forms of full-length CaM under these experimental conditions (Fig. 2, *F* and *L*) exhibited the same shapes and energies as the spectra for $CaM_{(76-148)}$.

In summary, excitation spectra monitored at 280 nm and emission spectra at an excitation wavelength of 250 nm showed that only the phenylalanine residues from $CaM_{(1-75)}$ contributed measurably to the emission at 280 nm. Consequently, the phenylalanine residues in the N-domain of $CaM_{(1-148)}$ are the only probes reporting calcium binding when this wavelength pair is used. This is best demonstrated by comparison of the emission spectra of the two domains in Fig. 2 *H* to those of the model amino acids in Fig. 2 *G*. It should be noted that although the C-domain has three phenylalanine residues (Phe89, Phe92, and Phe141), there was no detectable phenylalanine fluorescence from $CaM_{(76-148)}$ (Fig. 2 *H*). Using another pair of excitation and emission wavelengths, 277 and 320 nm, respectively, enabled the emission from the tyrosine residues in $CaM_{(76-148)}$ to be monitored without interference from phenylalanine emission (Fig. 2, *D*, *E*, *J*, and *K*). Consequently, by measuring the decrease in phenylalanine emission (with excitation at 250 nm and emission at 280 nm) and the increase in tyrosine emission (with excitation at 277 nm and emission at 320 nm), the binding of calcium to each domain could be measured separately. Importantly, because the spectra and calcium-dependent intensity changes of $CaM_{(1-148)}$ (Fig. 2, *C*, *F*, *I*, and *L*) closely resembled those of its two domain fragments, these two pairs of excitation and emission wavelengths could be used to resolve quantitatively the binding isotherms for each domain within the full-length protein.

Time-resolved fluorescence

For reference, intensity decays of three phenylalanine model compounds were examined. With excitation and emission at 250 and 280 nm, respectively, single-exponential decays were obtained for phenylalanine (as previously reported (Leroy et al., 1971; Duneau et al., 1998)), glycyl-phenylalanine, and *N*-acetyl-phenylalanine-amide at neutral pH. The lifetimes for these reference compounds were found to be 7.2, 5.9, and 4.8 ns, respectively.

Intensity decays corresponding to emission from phenylalanine residues were obtained for $CaM_{(1-75)}$ and $CaM_{(1-148)}$ by using the 250/280-nm wavelength pair for excitation and emission, respectively. As reported in Table 1, a sum of three exponential components was required to fit the data for each protein, either under apo or calcium-saturating conditions. For the apo forms of both $CaM_{(1-75)}$ and $CaM_{(1-148)}$, two lifetimes were shorter than those found for the phenylalanine model compounds, whereas the third was much longer. Addition of calcium to both proteins resulted in a decrease in the number and intensity average lifetimes. These decreases were consistent with the observed loss in steady-state intensities (Fig. 2). The most striking change in the individual decay parameters was the decrease in the long lifetime observed for both proteins, from 13.3 to 7.9 ns for $CaM_{(1-75)}$ and 11.8 to 6.3 ns for $CaM_{(1-148)}$. However, it should be noted that the decay profile for full-length CaM differed significantly from that for $CaM_{(1-75)}$ in both the apo and calcium-saturated forms. This was particularly evident in

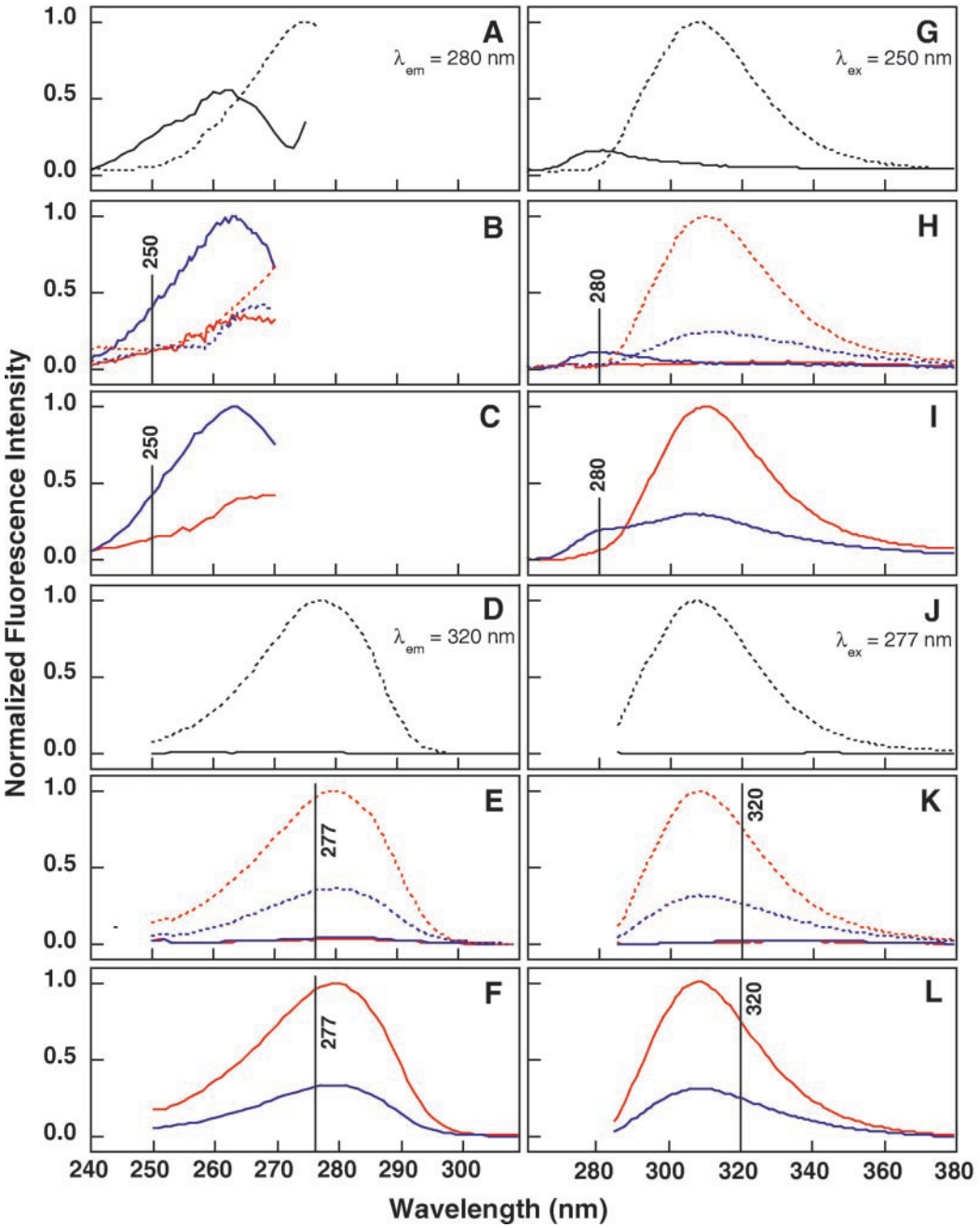

FIGURE 2 Normalized $[(f - f_{min})/(f_{max} - f_{min})]$ excitation (*A–F*) and emission (*G–L*) spectra of phenylalanine, tyrosine, $CaM_{(1–75)}$, $CaM_{(76–148)}$, and $CaM_{(1–148)}$. Proteins under calcium-saturated (*red*) and apo (*blue*) conditions are shown with lines indicating the wavelengths at which titrations are monitored. (*A–C*) λ_{em} = 280 nm; (*D–F*) λ_{em} = 320 nm: (*A*) Phenylalanine (*solid line*) and tyrosine (*dashed line*); (*B*) $CaM_{(1–75)}$ (*solid*) and $CaM_{(76–148)}$ (*dashed*); (*C*) $CaM_{(1–148)}$; (*D*) Phenylalanine (*solid*) and tyrosine (*dashed*); (*E*) $CaM_{(1–75)}$ (*solid*) and $CaM_{(76–148)}$ (*dashed*); (*F*) $CaM_{(1–148)}$. (*G—I*) λ_{ex} = 250 nm; (*J—L*) λ_{ex} = 277 nm: (*G*) Phenylalanine (*solid*) and tyrosine (*dashed*); (*H*) $CaM_{(1–75)}$ (*solid*) and $CaM_{(76–148)}$ (*dashed*); (*I*) $CaM_{(1–148)}$; (*J*) Phenylalanine (*solid*) and tyrosine (*dashed*); (*K*) $CaM_{(1–75)}$ (*solid*) and $CaM_{(76–148)}$ (*dashed*); (*L*) $CaM_{(1–148)}$.

the fractional intensities calculated from the recovered decay parameters (Table 1). This is consistent with studies that show that $CaM_{(1–75)}$ and the N-domain of $CaM_{(1–148)}$ have differences in some structural properties and in affinities of sites I and II (see Table 4) (Sorensen and Shea, 1998).

To study the fluorescence intensity decay of the tyrosine residues in $CaM_{(76–148)}$ and $CaM_{(1–148)}$, the 277/320-nm wavelength pair was used for excitation and emission, respectively. As reported in Table 2, a minimum of three exponential components was required to fit the data for each

TABLE 1 Fluorescence intensity decay parameters of $CaM_{(1-75)}$ and $CaM_{(1-148)}$ with 250-nm excitation and 280-nm emission

CaM	State	α_1^*	α_2^*	α_3^*	τ_1 (ns)†	τ_2 (ns)†	τ_3 (ns)†	f_1‡	f_2‡	f_3‡	$\langle\tau\rangle$ (ns)§	$\bar{\tau}$ (ns)¶
1-75	apo	0.53 (0.49, 0.58)	0.27 (0.23, 0.31)	0.20 (0.20, 0.20)	0.72 (0.68, 0.76)	1.81 (1.72, 1.92)	13.29 (13.20, 13.37)	10.9	14.2	74.9	10.3	3.5
1-75	Ca^{2+}	0.78 (0.74, 0.82)	0.16 (0.14, 0.17)	0.06 (0.06, 0.07)	0.57 (0.56, 0.58)	2.00 (1.92, 2.10)	7.88 (7.73, 8.01)	35.3	25.8	38.9	3.8	1.3
1-148	apo	0.43 (0.41, 0.47)	0.42 (0.39, 0.45)	0.14 (0.14, 0.15)	0.86 (0.81, 0.91)	2.46 (2.41, 2.53)	11.82 (11.68, 11.96)	11.8	33.4	54.8	7.4	3.1
1-148	Ca^{2+}	0.42 (0.40, 0.44)	0.52 (0.50, 0.53)	0.06 (0.06, 0.06)	0.53 (0.51, 0.56)	1.83 (1.81,1.85)	6.25 (6.06, 6.40)	14.4	61.7	23.9	2.7	1.5

*Amplitudes normalized to a sum of one; 95% confidence interval in parentheses (Straume et al., 1991).
†Fluorescence intensity lifetime; 95% confidence interval in parentheses.
‡Percent contribution to total intensity: $f_i = 100\ \alpha_i\tau_i/\Sigma\alpha_i\tau_i$.
§Intensity average lifetime: $\langle\tau\rangle = \Sigma\alpha_i\tau_i^2/\Sigma\alpha_i\tau_i$.
¶Number average lifetime: $\bar{\tau} = \Sigma\alpha_i\tau_i/\Sigma\alpha_i$.

protein either with or without calcium. The increase in average lifetimes upon saturation by calcium corresponded with the increase in steady-state fluorescence intensity (Fig. 2). Of interest, all decay parameters for both proteins, in either the apo or calcium-bound forms, were essentially the same, including the fractional intensities and average lifetimes (Table 2). Decay curves for $CaM_{(76-148)}$ and $CaM_{(1-148)}$ were also obtained with a 250/320-nm wavelength pair for excitation and emission, respectively. As reported in Table 3, the decay profiles of both proteins required three exponential components under apo and calcium-saturating conditions. Importantly, for each set of conditions, the decay parameters obtained for $CaM_{(76-148)}$ and $CaM_{(1-148)}$ were essentially the same at an emission wavelength of 320 nm when using either 250- or 277-nm excitation (i.e., number of average lifetimes near 1 and 2 ns for both apo- and calcium-bound forms, respectively, as indicated in Tables 2 and 3). This implied that emission from the phenylalanine residues in the N-domain of full-length CaM was not detected at 320 nm; the only emission was from tyrosine.

Equilibrium calcium titrations

Using the 250/280-nm excitation and emission wavelength pair to monitor phenylalanine fluorescence, $CaM_{(1-75)}$ underwent a calcium-dependent decrease in signal, as demonstrated previously (VanScyoc and Shea, 2001; Sorensen et al., 2002), whereas $CaM_{(76-148)}$ did not change in intensity throughout the entire titration (Fig. 3, *A* and *B*). The total free energy of calcium binding to sites I and II of $CaM_{(1-75)}$ was analyzed by nonlinear least-squares analysis (Eq. 3) (Sorensen and Shea, 1998; Shea et al., 2000; VanScyoc and Shea, 2001). The average of three trials was -13.9 ± 0.03 kcal/mol with an average cooperative free energy of -4.46 ± 0.72 kcal/mol (Table 4).

Tyrosine fluorescence (monitored using the 277/320-nm excitation and emission wavelength pair) of $CaM_{(76-148)}$ underwent a calcium-dependent increase in signal whereas the intensity of $CaM_{(1-75)}$ did not change over the entire titration (Fig. 3, *A* and *B*). Based on the average of three trials, the total free energy of calcium binding to sites III and IV of $CaM_{(76-148)}$ was -15.0 ± 0.06 kcal/mol, and the cooperative free energy was estimated as -2.37 ± 0.15 kcal/mol (Table 5).

Because all steady-state and time-resolved studies indicated that the 250/280-nm wavelength pair selectively monitored calcium binding to the N-domain sites of CaM whereas the 277/320-nm wavelength pair selectively monitored calcium binding to the C-domain sites of CaM, these two pairs of wavelengths were used to monitor both domains selectively within the full-length protein (Fig. 3 *C*). The average total free energy of calcium binding to sites I and II of $CaM_{(1-148)}$ was -13.4 ± 0.06 kcal/mol with a cooperative free energy of -1.28 ± 0.19 kcal/mol. The free

TABLE 2 Fluorescence intensity decay parameters of $CaM_{(76-148)}$ and $CaM_{(1-148)}$ with 277-nm excitation and 320-nm emission

CaM	State	α_1^*	α_2^*	α_3^*	τ_1 (ns)†	τ_2 (ns)†	τ_3 (ns)†	$f_1^\ddagger$	$f_2^\ddagger$	$f_3^\ddagger$	$\langle\tau\rangle$ (ns)§	$\bar{\tau}$ (ns)¶
76-148	apo	0.50 (0.49, 0.50)	0.46 (0.44, 0.47)	0.04 (0.04, 0.05)	0.33 (0.32, 0.35)	1.15 (1.14, 1.16)	3.67 (3.50, 3.80)	19.3	61.8	18.9	1.5	0.9
76-148	Ca^{2+}	0.14 (0.12, 0.15)	0.71 (0.69, 0.73)	0.16 (0.13, 0.18)	0.45 (0.38, 0.52)	1.99 (1.96, 2.02)	3.28 (3.17, 3.39)	3.1	71.2	25.7	2.3	2.0
1-148	apo	0.45 (0.44, 0.46)	0.46 (0.45, 0.46)	0.09 (0.09, 0.10)	0.31 (0.30, 0.31)	1.06 (1.05, 1.07)	2.56 (2.54, 2.58)	16.2	56.7	27.1	1.4	0.9
1-148	Ca^{2+}	0.14 (0.14, 0.15)	0.74 (0.74, 0.75)	0.11 (0.11, 0.12)	0.54 (0.51, 0.57)	2.09 (2.08, 2.09)	3.38 (3.34, 3.42)	3.9	77.1	19.0	2.3	2.0

*Amplitudes are normalized to a sum of one; 95% confidence intervals in parentheses (Straume et al., 1991).
†Fluorescence intensity lifetime; 95% confidence intervals in parentheses.
‡Percent contribution to total intensity: $f_i = 100\ \alpha_i\tau_i/\Sigma\alpha_i\tau_i$.
§Intensity average lifetime: $\langle\tau\rangle = \Sigma\alpha_i\tau_i^2/\Sigma\alpha_i\tau_i$.
¶Number average lifetime: $\bar{\tau} = \Sigma\alpha_i\tau_i/\Sigma\alpha_i$.

TABLE 3 Fluorescence intensity decay parameters of $CaM_{(76-148)}$ and $CaM_{(1-148)}$ with 250-nm excitation and 320-nm emission

CaM	State	α_1^*	α_2^*	α_3^*	τ_1 (ns)†	τ_2 (ns)†	τ_3 (ns)†	$f_1^\ddagger$	$f_2^\ddagger$	$f_3^\ddagger$	$\langle\tau\rangle$ (ns)§	$\bar{\tau}$ (ns)¶
76-148	apo	0.52 (0.51, 0.54)	0.41 (0.40, 0.42)	0.07 (0.06, 0.07)	0.35 (0.34, 0.36)	1.30 (1.28, 1.32)	4.13 (4.04, 4.20)	18.3	53.5	28.2	1.9	1.0
76-148	Ca^{2+}	0.19 (0.18, 0.22)	0.77 (0.74, 0.79)	0.04 (0.03, 0.04)	0.91 (0.83, 1.00)	2.19 (2.16, 2.22)	5.77 (5.43, 6.11)	8.4	81.5	10.1	2.5	2.1
1-148	apo	0.48 (0.46, 0.50)	0.45 (0.45, 0.46)	0.06 (0.06, 0.07)	0.38 (0.37, 0.39)	1.45 (1.43, 1.47)	4.86 (4.81, 4.91)	16.1	57.5	26.4	2.2	1.1
1-148	Ca^{2+}	0.18 (0.15, 0.22)	0.76 (0.71, 0.80)	0.05 (0.04, 0.07)	0.84 (0.71, 0.99)	2.07 (2.03, 2.11)	4.34 (4.08, 4.60)	7.8	79.8	12.4	2.3	2.0

*Amplitudes normalized to a sum of one; 95% confidence interval in parentheses (Straume et al., 1991).
†Fluorescence intensity lifetime; 95% confidence interval in parentheses.
‡Percent contribution to total intensity: $f_i = 100\ \alpha_i\tau_i/\Sigma\alpha_i\tau_i$.
§Intensity average lifetime: $\langle\tau\rangle = \Sigma\alpha_i\tau_i^2/\Sigma\alpha_i\tau_i$.
¶Number average lifetime: $\bar{\tau} = \Sigma\alpha_i\tau_i/\Sigma\alpha_i$.

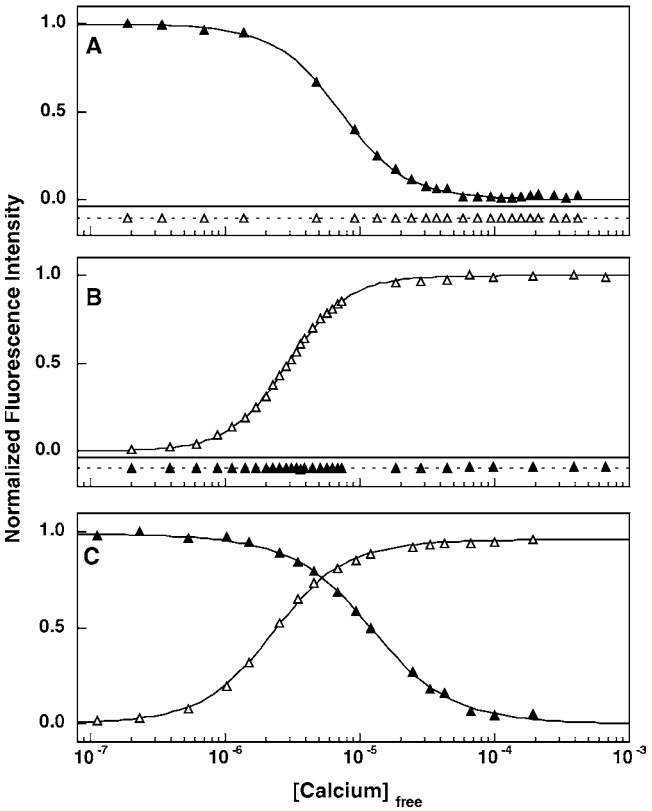

FIGURE 3 Calcium titrations of $CaM_{(1–148)}$ and domain fragments monitored at two pairs of wavelengths: λ_{ex} = 250 nm and λ_{em} = 280 nm (▲) and λ_{ex} = 277 nm and λ_{em} = 320 nm (△). (*A*) $CaM_{(1–75)}$; (*B*) $CaM_{(76–148)}$; (*C*) $CaM_{(1–148)}$. Data in each panel were normalized $[(f - f_{min})/(f_{max} - f_{min})]$. In *A* and *B*, the scale of the calcium-independent intensities was maintained, but the origin was offset to −0.1 to facilitate inspection.

energy of calcium binding to sites I and II in $CaM_{(1–148)}$ was less favorable than to these sites in the fragment $CaM_{(1–75)}$ ($\Delta\Delta G_2$ = 0.5 kcal/mol; Table 4). The average total free energy of calcium binding to sites III and IV in the C-domain of $CaM_{(1–148)}$ was −15.3 ± 0.07 kcal/mol with a cooperative free energy of −1.53 ± 0.07 kcal/mol (Table 5). Free energies determined for sites I and II and/or sites III and IV for $CaM_{(1–75)}$, $CaM_{(76–148)}$, and $CaM_{(1–148)}$ are in good agreement with previous determinations by proteolytic

TABLE 4 Free energies of calcium binding to sites I and II (250/280 nm)

Protein	ΔG_1^*	ΔG_2^*	$\Delta G_c^\dagger$	$\langle\sqrt{\text{var}}\rangle$
$CaM_{(1-75)}$‡	−5.46 ± 0.65	−13.9 ± 0.03	−4.46 ± 0.72	0.019
$CaM_{(1-148)}$	−6.44 ± 0.08	−13.4 ± 0.06	−1.28 ± 0.19	0.014
$R74A_{(1-148)}$	−6.62 ± 0.23	−13.8 ± 0.07	−1.37 ± 0.47	0.012
$R90A_{(1-148)}$	−6.56 ± 0.14	−13.4 ± 0.08	−1.29 ± 0.12	0.016
$R90G_{(1-148)}$	−6.91 ± 0.15	−13.6 ± 0.07	−1.11 ± 0.55	0.012

*Gibbs free energies (in kcal/mol (1 kcal = 4.184 kJ)) are described (Eq. 3). Free energies and errors represent averages and SDs between four trials.
†Estimate of cooperative free energy is described (Eq. 4).
‡Sorensen et al. (2002).

TABLE 5 Free energies of calcium binding to sites III and IV (277/320 nm)

Protein	ΔG_1^*	ΔG_2^*	$\Delta G_c^\dagger$	$\langle\sqrt{\text{var}}\rangle$
$CaM_{(76-148)}$	−6.74 ± 0.07	−15.0 ± 0.06	−2.37 ± 0.15	0.015
$CaM_{(1-148)}$	−7.28 ± 0.09	−15.3 ± 0.07	−1.53 ± 0.17	0.016
$R74A_{(1-148)}$	−7.23 ± 0.15	−15.3 ± 0.04	−1.68 ± 1.24	0.019
$R90A_{(1-148)}$	−6.82 ± 0.82	−15.6 ± 0.09	−2.03 ± 0.56	0.018
$R90G_{(1-148)}$	−7.55 ± 0.07	−15.7 ± 0.09	−0.46 ± 0.22	0.017

*Gibbs free energies (in kcal/mol (1 kcal = 4.184 kJ)) are described (Eq. 3). Free energies and errors represent averages and SDs between four trials.
†Estimate of cooperative free energy is described (Eq. 4).

footprinting (Pedigo and Shea, 1995a; Sorensen and Shea, 1998). For all calcium titrations, the standard deviations of the average ΔG_2 values for at least three trials (0.03–0.09 kcal/mol) were comparable to the confidence intervals for ΔG_2 determined from analysis of individual titrations (0.03–0.10 kcal/mol).

To explore the effects of mutating residues between sites II and III in $CaM_{(1–148)}$, calcium titrations of mutants R74A (end of helix D), R90A, and R90G (end of helix E) were conducted (Fig. 4; Tables 4 and 5). The mutation R74A caused an increase in affinity of sites I and II ($\Delta\Delta G_2$ of 0.4 kcal/mol) in the N-domain without affecting sites III and IV in the C-domain. The mutation R90A caused an increase in affinity of sites III and IV ($\Delta\Delta G_2$ of 0.3 kcal/mol) without affecting sites I and II in the N-domain. However, the mutation R90G caused an increase in affinity of sites I and II ($\Delta\Delta G_2$ of 0.2 kcal/mol) and sites III and IV ($\Delta\Delta G_2$ of 0.4 kcal/mol). Although these differences were small, they were judged to be significant because they were larger than 1) the standard deviation of the average of three or more trials for each mutant (see Tables and Fig. 5) and 2) the experimental error (confidence intervals) derived from nonlinear least-squares analysis of individual titration curves (which ranged from 0.03 to 0.10).

DISCUSSION

To the best of our knowledge, this is the first report of using phenylalanine fluorescence as an experimental observation of ligand-induced conformational change in a protein that contains both phenylalanine and tyrosine residues. In such proteins, phenylalanine fluorescence is likely to be quenched by resonance energy transfer to other aromatic residues, as the phenylalanine emission spectrum overlaps with their absorption (Chen, 1967; Eisinger et al., 1969; Eisinger, 1969; Lakowicz, 1999). The discovery that the calcium-dependent change in phenylalanine emission reports exclusively on conformational change in the N-domain has permitted us to monitor calcium binding to the two domains of calmodulin separately and determine whether mutations between sites II and III affected only one or both of the domains.

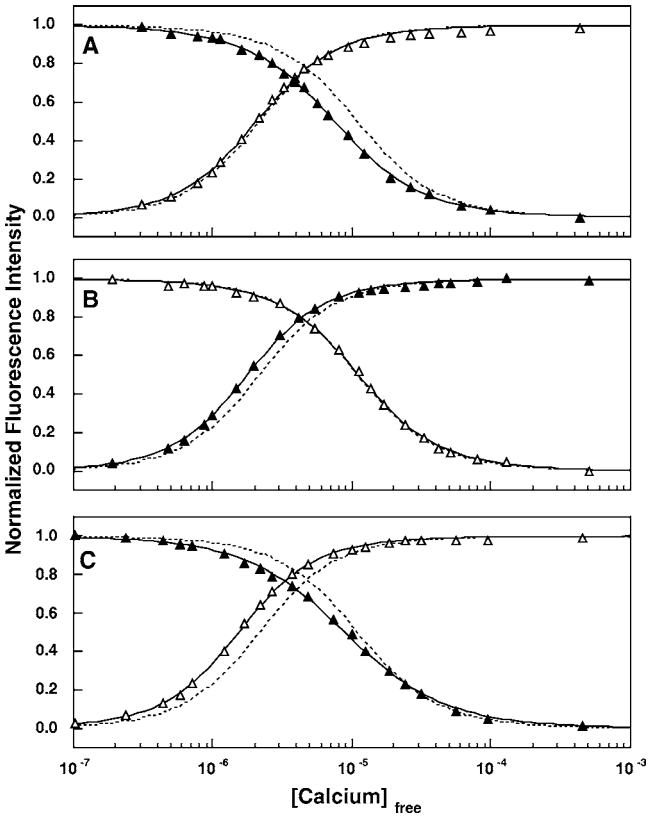

FIGURE 4 Calcium titrations of R74A $CaM_{(1–148)}$ (*A*), R90A $CaM_{(1–148)}$ (*B*), and R90G $CaM_{(1–148)}$ (*C*) monitored at two pairs of wavelengths: λ_{ex} = 250 nm and λ_{em} = 280 nm (▲) and λ_{ex} = 277 nm and λ_{em} = 320 nm (△). Data in each panel were normalized $[(f - f_{min})/(f_{max} - f_{min})]$. For comparison, the dashed line in each panel shows the fit for calcium binding to $CaM_{(1–148)}$.

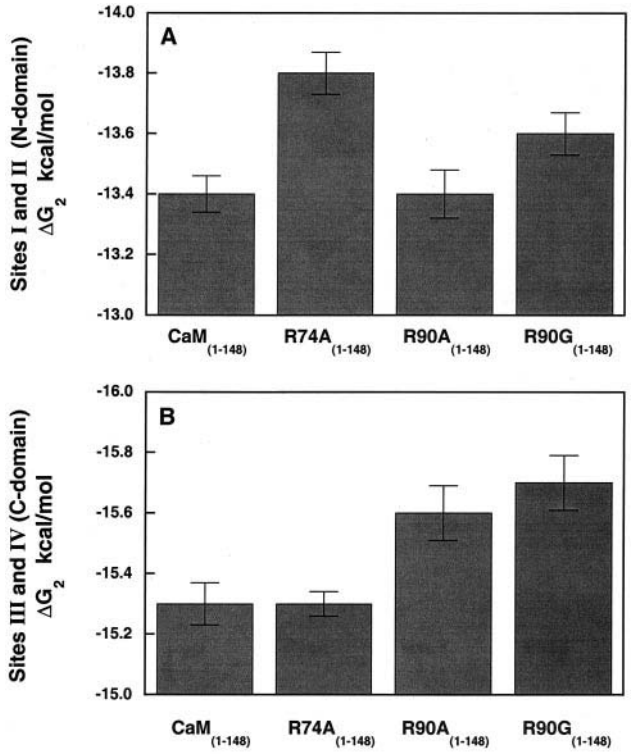

FIGURE 5 Comparison of the average total free energy (ΔG_2) of calcium binding to N-domain sites I and II (*A*) and C-domain sites III and IV (*B*) for $CaM_{(1–148)}$, R74A $CaM_{(1–148)}$, R90A $CaM_{(1–148)}$, and R90G $CaM_{(1–148)}$. Error bars indicate the SD for at least three trials.

Phenylalanine fluorescence is seldom used as a probe of conformation in proteins because of its weak emission compared with tyrosine or tryptophan, which in part is the result of its comparatively low extinction coefficient. Proteins known to contain phenylalanine as the only aromatic residue are rare but include parvalbumin from several species (Permyakov and Burstein, 1984; Sudhakar et al., 1993), peptides from epidermal growth factor receptor and ErbB-2 (Duneau et al., 1998), and the half-molecule N-domain of CaM (VanScyoc and Shea, 2001). All of these have been studied using phenylalanine fluorescence. To the best of our knowledge, this is the first report of the lifetimes of Phe residues in CaM.

Domain-specific titrations

For the first time, we have shown that it is possible to monitor calcium binding to each domain of CaM by intrinsic protein fluorescence. There is a clear separation between the calcium-dependent signal attributed to the phenylalanine residues in the N-domain and the signal from Tyr138 in the C-domain as shown by steady-state and time-resolved fluorescence studies of the apo and calcium-saturated states (Fig. 2; Tables 1–3). Calcium titrations of each half-molecule fragment ($CaM_{(1–75)}$ and $CaM_{(76–148)}$) monitored with excitation and emission wavelength pairs unique for phenylalanine and tyrosine show that the observable signals are selective for the N-domain and C-domain, respectively, throughout the entire transition from the apo to calcium-bound end-state (Fig. 3, *A* and *B*).

These studies demonstrate that conformational change in each domain of the full-length molecule ($CaM_{(1–148)}$) can be monitored separately by domain-specific fluorescence spectroscopy (Fig. 3 *C*). Phenylalanine residues in the N-domain can be monitored with an excitation and emission wavelength pair of 250/280 nm to report exclusively on the calcium occupancy of sites I and II. There is no contribution to the signal from phenylalanine residues in the C-domain, no spectral interference from the tyrosine residues in the C-domain, and no observable energy transfer from the N-domain phenylalanine residues to the C-domain tyrosine residues. As recognized previously, Tyr in the C-domain can be used to monitor the calcium occupancy of sites III and IV with the excitation/emission wavelength pair of 277/320 nm (Richman and Klee, 1979; Klevit, 1983; Larson et al., 1990; Ross et al., 1992) with no interference from the phenylalanine residues in the N-domain.

These domain-specific signals were used to monitor the effects of mutating R74 and R90, two highly conserved residues outside of the calcium-binding sites, on calcium affinity. In a comparison of CaM from over 50 nonfungi species, residue 74 was found to be Arg in all cases but four. Residue 90 was found to be arginine in about half of the cases and lysine in the other half, and there was one occurrence of glutamine. On the basis of molecular dynamics simulations, these residues were postulated to have long-range effects on the tertiary structure of $(Ca^{2+})_4$-CaM (Pascual-Ahuir et al., 1991), mediating tertiary structural changes (Weinstein and Mehler, 1994). In this study, both arginine residues were substituted by alanine, a residue with high helical propensity and at position 90, also by glycine, a residue often found in turns.

Calcium-binding titrations (Fig. 4) showed that mutation of these residues increased the calcium affinity of sites in one or both of the domains. Substitution of alanine for either R74 at the end of helix D in the N-domain or R90 at the end of helix E in the C-domain increased only the affinity of the domain containing the mutation. However, substitution of glycine for R90 increased the affinity of calcium-binding sites in both the N- and C-domain. Previous studies demonstrated that all of these mutations increased the Stokes radius relative to wild-type CaM (Sorensen and Shea, 1996). However, the smallest changes were caused by substitution of alanine (R74A showed a 0.16-Å increase and R90A showed a 0.57-Å increase) whereas R90G caused a 1.02-Å increase in Stokes radius when compared with wild-type CaM. This correlation between increased affinity and increased Stokes radius was also observed with N-domain fragments of mutants of *Paramecium* $CaM_{(1–75)}$ (VanScyoc and Shea, 2001). These findings suggest that an increase in disorder can contribute to an increase in affinity of the calcium-binding sites, presumably by lowering tertiary constraints on rearrangements needed for optimal coordination of the divalent cation in each site.

Long phenylalanine lifetime diagnostic of the N-domain

One of the three lifetimes resolved for phenylalanine fluorescence of apo $CaM_{(1–75)}$ (13.3 ns) was significantly longer than any of the lifetimes (7.2–4.8 ns) resolved for the Phe model compounds (phenylalanine, glycyl-phenylalanine, or N-acetyl-phenylalanine-amide). A similarly long lifetime (11.8 ns) was observed for apo $CaM_{(1–148)}$. This long lifetime serves as a marker for the apo N-domain and suggests that one or more of its Phe residues is in a distinctive environment in both $CaM_{(1–75)}$ and $CaM_{(1–148)}$. In CaM, upon saturation of sites I and II by calcium, the resulting conformational changes must alter the local environment of the unique phenylalanine residue(s) to reduce the long lifetime (from 13.3 to 7.9 ns in the domain fragment and from 11.8 to 6.2 ns in the full-length molecule). The lifetimes under calcium-saturating condition are similar to those observed for the model compounds.

The long lifetimes found for the N-domain of CaM may be compared to an analysis of the intensity decay of phenylalanine in parvalbumin (another EF-hand calcium-binding protein). It was biexponential in the calcium-saturated state with lifetimes of 5.9 and 53 ns and monoexponential in the apo state with a lifetime of 17 ns (Sudhakar et al., 1993). That study offers precedence for a long lifetime for Phe in a protein environment. The low extinction coefficient of the phenylalanine side chain is a reflection of both low absorption and emission transition probabilities compared with tyrosine or tryptophan. Thus, it is to be expected that long fluorescence lifetimes have been observed for phenylalanine in proteins.

Because the N-domain contains five phenylalanine residues, it is not possible to assign individual fluorescence lifetimes to specific residues unequivocally. However, it is possible to compare calcium-dependent differences in the positions of the rings of Phe residues in the N-domain of apo CaM (1CFD.pdb) (Kuboniwa et al., 1995) to those in calcium-saturated CaM (3CLN.pdb) (Babu et al., 1988). As shown in Fig. 6, *A* and *B*, the calcium-dependent changes in the pair-wise separations between Phe12, Phe16, Phe65, and Phe68 are small (the center-to-center ring distance shifts range from 0.1 to 0.4 Å). In contrast, distances between Phe19 and each of the other four phenylalanine residues are reduced considerably by calcium binding. They shorten by 1.7 Å (to Phe12), 0.6 Å (to Phe16), 1.1 Å (to Phe65), and 3.8 Å (to Phe68). This suggests that the fluorescence of Phe19 is the major contributor to the long-lifetime component observed in CaM and that its intensity is quenched dynamically as it joins the network formed by the other four phenylalanine side chains. Upon binding of calcium to sites I and II, Phe19 also becomes more solvent exposed, as do the other phenylalanine residues, as determined by measuring the solvent-accessible surface area of structures of apo (1CFD.pdb) ((Kuboniwa et al., 1995) and calcium-saturated (3CLN.pdb) ((Babu et al., 1988) CaM. This is consistent with its lifetime becoming more similar to those observed for phenylalanine in small model compounds in aqueous solvents.

Phenylalanine-to-tyrosine Förster resonance energy transfer

Individual and average lifetimes were slightly longer for the 250/320-nm pair than the 277/320-nm pair for both $CaM_{(76–148)}$ and $CaM_{(1–148)}$ (Tables 2 and 3). This may indicate that there is resonance energy transfer within the C-domain from its three phenylalanine residues (89, 92, and 141) to tyrosine. The Förster distance for 50% resonance energy transfer from phenylalanine to tyrosine is ~10 Å in peptides (Eisinger et al., 1969; Eisinger, 1969) and proteins (Searcy et al., 1989). Center-to-center ring distances between Tyr138 and the Phe residues in the C-domain are 5.1

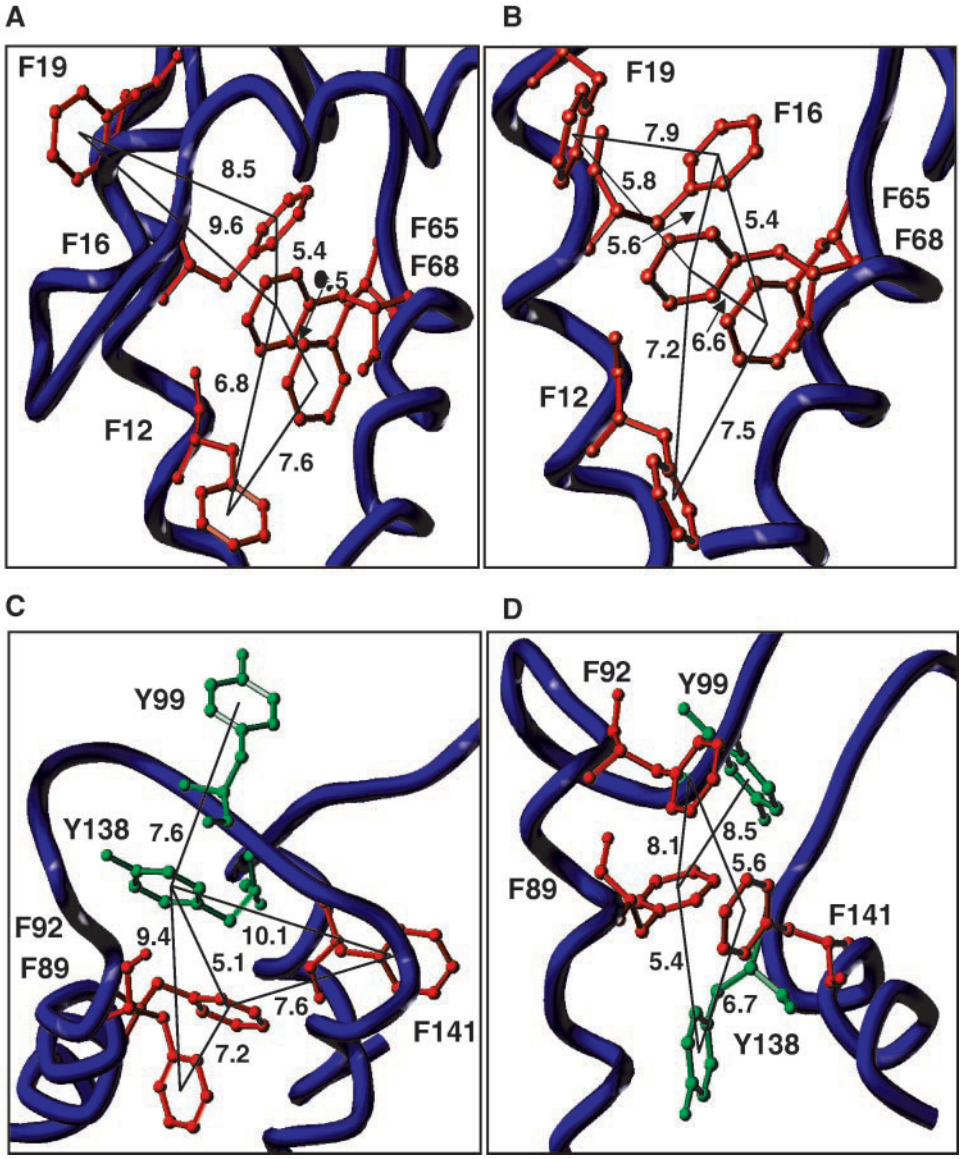

FIGURE 6 Orientation of phenylalanine (*red*) and tyrosine (*green*) residues in CaM. (*A*) Apo N-domain (residues 1–75 from 1CFD.pdb shown (Kuboniwa et al., 1995)); (*B*) Calcium-saturated N-domain (residues 1–75 from 3CLN.pdb shown (Babu et al., 1988)); (*C*) Apo C-domain (residues 76–148 from 1CFD.pdb shown); (*D*) Calcium-saturated C-domain (residues 76–148 from 3CLN.pdb shown). Models were drawn using SYBYL (Tripos).

Å (to Phe89), 9.4 Å (to Phe92), and 10.1 Å (to Phe141) in the apo state (1CFD.pdb) (Kuboniwa et al., 1995) and change to 5.4 Å, 6.7 Å, and 11.7 Å in the calcium-saturated state (3CLN.pdb) (Babu et al., 1988) (Fig. 6, *C* and *D*). It is reasonable that these moderately small distances allow for transfer of energy from phenylalanine to tyrosine, thereby helping quench these C-domain phenylalanine residues in both $CaM_{(76–148)}$ and $CaM_{(1–148)}$ (i.e., in a manner independent of the N-domain).

In contrast, distances between the Phe residues in the N-domain and Tyr138 in the C-domain are much longer. The inter-ring distance between Tyr138 (in the C-domain) and Phe12 (the closest phenylalanine in the N-domain) is 25.1 Å in the calcium-saturated structure (3CLN.pdb; (Babu et al., 1988)). In the absence of calcium (1CFD.pdb; (Kuboniwa et al., 1995), that distance extends to 28.3 Å. Distances of 25 Å or greater are more than twice the Förster distance, and the energy transfer efficiency, which depends on the sixth power of the distance, effectively will be zero. Therefore, it is unlikely that N-domain phenylalanine residues transfer excitation energy to the tyrosine residues in the C-domain.

Effect of the N-domain on tyrosine environment

The time-resolved studies revealed similar tyrosine emission decay profiles for $CaM_{(76–148)}$ and $CaM_{(1–148)}$, both in

the presence and absence of calcium. To help evaluate whether they were indistinguishable, decay data for both proteins were analyzed together by a global procedure (Beechem et al., 1983; Knutson et al., 1983). The equivalent amplitudes recovered for the common lifetimes confirm that the tyrosine intensity decays of $CaM_{(76–148)}$ and $CaM_{(1–148)}$ are completely indistinguishable in both the apo and calcium-bound forms (data not shown). This indicates that covalent linkage to the N-domain does not cause a significant perturbation of tyrosine environments within $CaM_{(1–148)}$. There is also little effect of the N-domain on calcium-binding properties of the C-domain, as the calcium affinities of sites III and IV are nearly identical for the two molecules ($CaM_{76–148}$ and $CaM_{1–148}$), as shown in Table 5. Consequently, based on fluorescence properties and calcium binding, it would appear that the interactions between the N-domain and C-domain do not induce significant structural perturbations within the C-domain. This finding also agrees with comparative studies of CaM and its C-domain fragment by flow dialysis (Klee, 1988), chelator methods (Martin et al., 1985; Linse et al., 1991), and proteolytic footprinting (Sorensen and Shea, 1998).

The effect of the C-domain on the N-domain is currently being investigated. There are differences in structural properties and in affinities of sites I and II between the N-domain of full-length CaM and $CaM_{(1–75)}$ (Table 4) (Sorensen and Shea, 1998; Sorensen et al., 2002) that are reflected by slight differences in lifetimes between the two proteins (Table 1). However, the data presented here unequivocally demonstrate that the fluorescence signal obtained by exciting CaM at 250 nm and monitoring emission at 280 nm reports on the occupancy of sites I and II. This finding has allowed us to determine directly how mutations between sites II and III may affect one or both domains, depending on the nature of the substitution.

Summary

This new technique for determining macroscopic binding constants for the N-domain sites I and II and the C-domain sites III and IV of CaM with intrinsic fluorescence should prove applicable to most species of calmodulin because its sequence is highly conserved across the animal and plant kingdoms (e.g., rat CaM is identical to human and bovine CaM, 97% identical to *Drosophila* CaM, 88% identical to *Paramecium* CaM, and 90% identical to alfalfa CaM). Only 1 of over 50 species of CaM (*Mougeotia scalaris*, an alga) naturally contains Trp (found at position 105 in the C-domain); its properties would need to be explored independently.

The method described here alleviates the need to introduce mutations or extrinsic reporter groups. It does not require comparison between the calcium-binding properties of full-length CaM to fragments of CaM to assign equilibrium constants. This new technique will make it easier to explore why the two highly homologous domains differ significantly in calcium-binding affinity and thermostability despite their structural similarity. This approach will also be valuable for studying mutants in which there are small differences between the free energies of calcium binding to sites in the C-domain and sites in the N-domain (Beckingham, 1991; Shea et al., 1996; Jaren et al., 2000). Although other studies have indicated the importance of residues within the binding sites proper (Renner et al., 1993; Drake et al., 1997), the mutants studied here illustrate that distant residues may tune calcium binding, even in the opposite domain.

There are also potential applications for using these intrinsic, domain-specific reporters to explore calcium-binding properties of multi-protein complexes of CaM given that the two domains have unique roles in activation of some target proteins (Kung et al., 1992; Ohya and Botstein, 1994; Schumacher et al., 2001; Rodney et al., 2001). This study of CaM raises the possibility that other multi-domain proteins that contain both Phe and Tyr may be amenable for study in the same fashion, permitting resolution of domain-specific properties of ligand-induced conformational switching.

We thank Lynn Teesch and Elena Rus for amino acid analysis (University of Iowa College of Medicine, Molecular Analysis Facility).

These studies were supported by a grant to M.A.S. from the National Institutes of Health (RO1 GM 57001), a fellowship to W.S.V. from the University of Iowa Center for Biocatalysis and Bioprocessing, a grant to W.R.L. from The National Science Foundation (DBI-9724330), and grants to J.B.A.R. from the National Institutes of Health (HL29019 and CA63317).

REFERENCES

Ababou, A., and J. R. Desjarlais. 2001. Solvation energetics and conformational change in EF-hand proteins. *Protein Sci.* 10:301–312.

Babu, Y. S., C. E. Bugg, and W. J. Cook. 204. 1988. Structure of calmodulin refined at 2.2 Å resolution. *J. Mol. Biol.*191–204.

Beckingham, K. 1991. Use of site-directed mutations in the individual Ca^{2+}-binding sites of calmodulin to examine Ca^{2+}-induced conformational changes. *J. Biol. Chem.* 266:6027–6030.

Beechem, J. M., J. R. Knutson, J. B. A. Ross, B. W. Turner, and L. Brand. 1983. Global resolution of heterogeneous decay by phase/modulation fluorometry: mixtures and proteins. *Biochemistry.* 22:6054–6058.

Bevington, P. R. 1969. Data Reduction and Error Analysis for the Physical Sciences. McGraw-Hill, New York.

Buccigross, J. M., C. L. O'Donnel, and D. J. Nelson. 1986. A flow-dialysis method for obtaining relative measures of association constants in calmodulin-metal-ion systems. *Biochem. J.* 235:677–684.

Carafoli, E., and C. Klee. 1999. Calcium as a cellular regulator. Oxford University Press, New York.

Chattopadhyaya, R., W. E. Meador, A. R. Means, and F. A. Quiocho. 1992. Calmodulin structure refined at 1.7 Å resolution. *J. Mol. Biol.* 228: 1177–1192.

Chen, R. F. 1967. Fluorescence quantum yields of tryptophan and tyrosine. *Anal. Lett.* 1:35–42.

Crivici, A., and M. Ikura. 1995. Molecular and structural basis of target recognition by calmodulin. *Annu. Rev. Biophys. Biomol. Struct.* 24: 85–116.

Drake, S. K., M. A. Zimmer, C. L. Miller, and J. J. Falke. 1997. Optimizing the metal binding parameters of an EF-hand-like calcium chelation loop: coordinating side chains play a more important tuning role than chelation loop flexibility. *Biochemistry.* 36:9917–9926.

Duneau, J. P., N. Garnier, G. Cremel, G. Nullans, P. Hubert, D. Genest, M. Vincent, J. Gallay, and M. Genest. 1998. Time resolved fluorescence properties of phenylalanine in different environments: comparison with molecular dynamics simulation. *Biophys. Chem.* 73:109–119.

Eisinger, J. 1969. A variable temperature, U.V. luminescence spectrograph for small samples. *Photochem. Photobiol.* 9:247–258.

Eisinger, J., B. Feuer, and A. A. Lamola. 1969. Intramolecular singlet excitation transfer: applications to polypeptides. *Biochemistry*. 8:3908–3915.

Gilli, R., D. Lafitte, C. Lopez, M. Kilhoffer, A. Makarov, C. Briand, and J. Haiech. 1998. Thermodynamic analysis of calcium and magnesium binding to calmodulin. *Biochemistry.* 37:5450–5456.

Grinvald, A., and I. Z. Steinberg. 1974. On the analysis of fluorescence decay kinetics by the method of least squares. *Anal. Biochem.* 59: 583–598.

Haiech, J., C. B. Klee, and J. G. Demaille. 1981. Effects of cations on affinity of calmodulin for calcium: ordered binding of calcium ions allows the specific activation of calmodulin-stimulated enzymes. *Biochemistry*. 20:3890–3897.

Haiech, J., B. Vallet, R. Aquaron, and J. G. Demaille. 1980. Ligand binding to macromolecules: determination of binding parameters by combined use of ligand buffers and flow dialysis: application to calcium-binding proteins. *Anal. Biochem.* 105:18–23.

Ikura, M., T. Hiraoki, K. Hikichi, T. Mikuni, M. Yazawa, and K. Yagi. 1983. Nuclear magnetic resonance studies on calmodulin: calcium-induced conformational change. *Biochemistry.* 22:2573–2579.

Jaren, O. R., S. Harmon, A. F. Chen, and M. A. Shea. 2000. *Paramecium* calmodulin mutants defective in ion channel regulation can bind calcium and undergo calcium-induced conformational switching. *Biochemistry.* 39:6881–6890.

Kilhoffer, M.-C., M. Kubina, F. Travers, and J. Haiech. 1992. Use of engineered proteins with internal tryptophan reporter groups and pertubation techniques to probe the mechanism of ligand-protein interactions: investigation of the mechanism of calcium binding to calmodulin. *Biochemistry.* 31:8098–8106.

Klee, C. B. 1988. Interaction of calmodulin with Ca^{2+} and target proteins. *In* Calmodulin. Elsevier, New York. 35–56.

Klevit, R. E. 1983. Spectroscopic analyses of calmodulin and its interactions. *Methods Enzymol.* 102:82–104.

Klevit, R. E., D. C. Dalgarno, B. A. Levine, and R. J. P. Williams. 1984. ^{1}H-NMR studies of calmodulin: the nature of the Ca^{2+}-dependent conformational change. *Eur. J. Biochem.* 139:109–114.

Knutson, J. R., J. M. Beechem, and L. Brand. 1983. Simultaneous analysis of multiple fluorescence decay curves: a global approach. *Chem. Phys. Lett.* 102:501–507.

Kuboniwa, H., N. Tjandra, S. Grzesiek, H. Ren, C. B. Klee, and A. Bax. 1995. Solution structure of calcium-free calmodulin. *Nat. Struct. Biol.* 2:768–776.

Kung, C., R. R. Preston, M. E. Maley, K.-Y. Ling, J. A. Kanabrocki, B. R. Seavey, and Y. Saimi. 1992. In vivo *Paramecium* mutants show that calmodulin orchestrates membrane responses to stimuli. *Cell Calcium.* 13:413–425.

Lakowicz, J. R. 1999. Principles of Fluorescence Spectroscopy, 2nd ed. Kluwer Academic/Plenum Publishing, New York.

LaPorte, D. C., B. M. Wierman, and D. R. Storm. 1980. Calcium-induced exposure of a hydrophobic surface on calmodulin. *Biochemistry.* 19: 3814–3819.

Larson, R. E., F. S. Espindola, and E. M. Espreafico. 1990. Calmodulin-binding proteins and calcium/calmodulin regulated enzyme activities associated with brain actomyosin. *J. Neurochem.* 54:1288–1294.

Leroy, E., H. Lami, and G. Laustriat. 1971. Fluorescence lifetime and quantum yield of phenylalanine aqueous solutions: temperature and concentration effects. *Photochem. Photobiol.* 13:411–421.

Linse, S., A. Helmersson, and S. Forsén. 1991. Calcium binding to calmodulin and its globular domains. *J. Biol. Chem.* 266:8050–8054.

Malmendal, A., S. Linse, J. Evenäs, S. Forsen, and T. Drakenberg. 1999. Battle for the EF-hands: magnesium-calcium interference in calmodulin. *Biochemistry.* 38:11844–11850.

Martin, S. R., A. Andersson-Teleman, P. M. Bayley, T. Drakenberg, and S. Forsén. 1985. Kinetics of calcium dissociation from calmodulin and its tryptic fragments: a stopped-flow fluorescence study using Quin 2 reveals a two-domain structure. *Eur. J. Biochem.* 151:543–550.

Martin, S. R., P. M. Bayley, S. E. Brown, T. Porumb, M. Zhang, and M. Ikura. 1996. Spectroscopic characterization of a high-affinity calmodulin-target peptide hybrid molecule. *Biochemistry.* 35:3508–17. .

Martin, S. R., L. Masino, and P. M. Bayley. 2000. Enhancement by Mg^{2+} of domain specificity in Ca^{2+}-dependent interactions of calmodulin with target sequences. *Protein Sci.* 9:2477–2488.

Nelson, M. R., and W. J. Chazin. 1998. An interaction-based analysis of calcium-induced conformational changes in Ca^{2+} sensor proteins. *Protein Sci.* 7:270–282. .

Nomura, M., J. T. Stull, K. E. Kamm, and M. C. Mumby. 1992. Site-specific dephosphorylation of smooth muscle myosin light chain kinase by protein phosphatases 1 and 2A. *Biochemistry.* 31:11915–20.

Ohya, Y., and D. Botstein. 1994. Diverse essential functions revealed by complementing yeast calmodulin mutants. *Science.* 263:963–966.

Pascual-Ahuir, J.-L., E. L. Mehler, and H. Weinstein. 1991. Calmodulin structure and function: implication of arginine in the compaction related to ligand binding. *Mol. Eng.* 1:231–247.

Pedigo, S., and M. A. Shea. 1995a. Discontinuous equilibrium titrations of cooperative calcium binding to calmodulin monitored by 1-D ^{1}H-nuclear magnetic resonance spectroscopy. *Biochemistry.* 34:10676–10689.

Pedigo, S., and M. A. Shea. 1995b. Quantitative endoproteinase GluC footprinting of cooperative Ca^{2+} binding to calmodulin: proteolytic susceptibility of E31 and E87 indicates interdomain interactions. *Biochemistry.* 34:1179–1196.

Permyakov, E. A., and E. A. Burstein. 1984. Some Aspects of studies of thermal transitions in proteins by means of their intrinsic fluorescence. *Biophys. Chem.* 19:265–271.

Putkey, J. A., G. R. Slaughter, and A. R. Means. 1985. Bacterial expression and characterization of proteins derived from the chicken calmodulin cDNA and a calmodulin processed gene. *J. Biol. Chem.* 260: 4704–4712.

Renner, M., M. A. Danielson, and J. J. Falke. 1993. Kinetic control of Ca(II) signaling: tuning the ion dissociation rates of EF-hand Ca(II) binding sites. *Proc. Natl. Acad. Sci. U.S.A.* 90:6493–6497.

Richman, P. G., and C. B. Klee. 1979. Specific perturbation by Ca^{2+} of tyrosyl residue 138 of calmodulin. *J. Biol. Chem.* 254:5372–5376.

Rodney, G. G., C. P. Moore, B. Y. Williams, J. Z. Zhang, J. Krol, S. E. Pedersen, and S. L. Hamilton. 2001. Calcium binding to calmodulin leads to an N-terminal shift in its binding site on the ryanodine receptor. *J. Biol. Chem.* 276:2069–2074. .

Ross, J. B. A., W. R. Laws, K. W. Rousslang, and H. R. Wyssbrod. 1992. Tyrosine fluorescence and phosphorescence from proteins and polypeptides. *In* Topics in Fluorescence Spectroscopy, Vol. 3: Biochemical Applications. Plenum Press, New York. 1–63.

Schumacher, M. A., A. F. Rivard, H. P. Bachinger, and J. P. Adelman. 2001. Structure of the gating domain of a Ca^{2+}-activated K^+ channel complexed with Ca^{2+}/calmodulin. *Nature.* 410:1120–1124.

Seamon, K. B. 1980. Calcium- and magnesium-dependent conformational states of calmodulin as determined by nuclear magnetic resonance. *Biochemistry.* 19:207–215.

Searcy, D. G., T. Montenay-Garestier, and C. Hélène. 1989. Phenylalanine-to-tyrosine singlet energy transfer in archaebacterial histone-like protein HTa. *Biochemistry.* 28:9058–9065.

Shea, M. A., B. R. Sorensen, S. Pedigo, and A. Verhoeven. 2000. Proteolytic footprinting titrations for estimating ligand-binding constants and detecting pathways of conformational switching of calmodulin. *Methods Enzymol.* 323:254–301.

Shea, M. A., A. S. Verhoeven, and S. Pedigo. 1996. Calcium-induced interactions of calmodulin domains revealed by quantitative thrombin footprinting of Arg37 and Arg106. *Biochemistry*. 35:2943–2957.

Sorensen, B. R., L. A. Faga, R. Hultman, and M. A. Shea. 2002. Interdomain linker increases thermostability and decreases calcium affinity of calmodulin N-domain. *Biochemistry*. 41:15–20.

Sorensen, B. R., and M. A. Shea. 1996. Calcium binding decreases the Stokes radius of calmodulin and mutants R74A, R90A, and R90G. *Biophys. J.* 71:3407–3420.

Sorensen, B. R., and M. A. Shea. 1998. Interactions between domains of Apo calmodulin alter calcium binding and stability. *Biochemistry*. 37: 4244–4253.

Straume, M., S. G. Fraiser-Cadoret, and M. L. Johnson. 1991. Least-squares analysis of fluorescence data. *In* Topics in Fluorescence Spectroscopy, Vol. 2: Principles. Plenum Press, New York. 177–240.

Strynadka, N. C. J., and M. N. G. James. 1989. Crystal structures of the helix-loop-helix calcium-binding proteins. *Annu. Rev. Biochem.* 58: 951–998.

Sudhakar, K., W. W. Wright, S. A. Williams, C. M. Phillips, and J. M. Vanderkooi. 1993. Phenylalanine fluorescence and phosphorescence used as a probe of conformation for cod parvalbumin. *J. Fluoresc.* 3:57–64.

Tikunova, S. B., D. J. Black, J. D. Johnson, and J. P. Davis. 2001. Modifying Mg^{2+} binding and exchange with the N-terminal of calmodulin. *Biochemistry*. 40:3348–3353. .

VanScyoc, W. S., and M. A. Shea. 2001. Phenylalanine fluorescence studies of calcium binding to N-domain fragments of *Paramecium* calmodulin mutants show increased calcium affinity correlates with increased disorder. *Protein Sci.* 10:1758–1768.

Waltersson, Y., S. Linse, P. Brodin, and T. Grundström. 1993. Mutational effects on the cooperativity of Ca^{2+} binding in calmodulin. *Biochemistry.* 32:7866–7871.

Wang, C.-L. A. 1985. A note on Ca^{2+} binding to calmodulin. *Biochem. Biophys. Res. Commun.* 130:426–430.

Weinstein, H., and E. L. Mehler. 1994. Ca^{2+}-binding and structural dynamics in the functions of calmodulin. *Annu. Rev. Physiol*. 56:213–236.

Yao, Y., C. Schöneich, and T. C. Squier. 1994. Resolution of structural changes associated with calcium activation of calmodulin using frequency domain fluorescence spectroscopy. *Biochemistry*. 33: 7797–7810.

Yap, K. L., J. B. Ames, M. B. Swindells, and M. Ikura. 1999. Diversity of Conformational States and Changes Within the EF-Hand Protein Superfamily. *Proteins.* 37:499–507.